Distribution of Arctic and Pacific copepods and their habitat in the northern Bering and Chukchi Seas

H. Sasaki[1, 2], K. Matsuno[1, 2], A. Fujiwara[3], M. Onuka[4], A. Yamaguchi[2], H. Ueno[2], Y. Watanuki[2] and T. Kikuchi[3]

[1] {Arctic Environment Research Center, National Institute of Polar Research, 10-3 Midori-cho, Tachikawa, Tokyo 190-8518, Japan}

[2] {Graduate School of Fisheries Sciences, Hokkaido University, 3-1-1 Minato-cho, Hakodate, Hokkaido 041-8611, Japan}

[3] {Japan Agency for Marine-Earth Science and Technology, 2-15 Natsushima-cho, Yokosuka, Kanagawa 237-0061, Japan}

[4] {Graduate School of Environmental Science, Hokkaido University, N10W5, Sapporo, Hokkaido 060-0810, Japan}

Correspondence to: H.Sasaki (hiro_sasaki@salmon.fish.hokudai.ac.jp)

Abstract

The advection of warm Pacific water and the reduction in sea ice in the western Arctic Ocean may influence the abundance and distribution of copepods, a key component of food webs. To quantify the factors affecting the abundance of copepods in the northern Bering and Chukchi Seas, we constructed habitat models explaining the spatial patterns of large and small Arctic and Pacific copepods, separately. Copepods were sampled using NORPAC nets. The structures of water masses indexed by using principle component analysis scores, satellite-derived timing of sea ice retreat, bottom depth, and chlorophyll *a* concentration were integrated into generalized additive models as explanatory variables. The adequate models for all copepods exhibited clear continuous relationships between the abundance of copepods and the indexed water masses. Large Arctic copepods were abundant at stations where the bottom layer was saline; however they were scarce at stations where warm fresh water formed the upper layer. Small Arctic copepods were abundant at stations where the upper layer was warm and saline and the bottom layer was cold and highly saline. In contrast, Pacific

copepods were abundant at stations where the Pacific-origin water mass was predominant (i.e. a warm, saline upper layer and saline and a highly saline bottom layer). All copepod groups showed a positive relationship with early sea ice retreat. Early sea ice retreat has been reported to initiate spring blooms in open water, allowing copepods to utilize more food while maintaining their high activity in warm water without sea ice and cold water. This finding indicates that early sea ice retreat has positive effects on the abundance of all copepod groups in the northern Bering and Chukchi Seas, suggesting a change from a pelagic–benthic-type ecosystem to a pelagic–pelagic type.

1 Introduction

Over the last decade, seasonal sea ice coverage has changed dramatically in the northern Bering and Chukchi Seas (Comiso et al., 2008; Parkinson and Comiso, 2012), possibly because of an increase in the inflow of Pacific water from the Bering Sea through the Bering Strait (Shimada et al., 2006). The Bering Strait is shallow (<30 m) and has a gentle shelf extending to the Arctic Shelf break through the Chukchi Sea. On this extensive shallow shelf, the food webs are short and efficient, and even small changes in production pathways can affect organisms at higher trophic levels (Grebmeier et al., 2006). The recent change in the sea ice melt timing contributes to stratification, nutrient trapping at the surface, and lower primary production with insufficient sunlight (Clement, 2004). In contrast, it has been suggested that the timing of the phytoplankton bloom has also altered (Kahru et al., 2011) and that its annual primary production has increased (Arrigo et al., 2008). Changes in the timing and location of primary production and associated grazing by zooplankton have a direct influence on the energy and matter transfer to the benthic community (Grebmeier et al., 2010).

In the Bering and Chukchi Seas, several water masses have been identified based on their basis of salinity and temperature (Table 1). The water masses include the relatively warm/low-salinity Alaskan coastal water (ACW; temperature 2.0–13.0 °C and salinity <31.8) that originates from the eastern Bering Sea; the warm/saline Bering shelf water (BSW; 0.0–10.0 °C and 31.8–33.0) from the middle Bering shelf; and the cold/higher-salinity Anadyr water (AW; −1.0–1.5 °C and 32.3–33.3) originating from the Gulf of Anadyr at depth along the continental shelf of the Bering Sea. The BSW and AW merge to form the Bering Sea Anadyr water (BSAW; Coachman et al., 1975; Springer et al., 1989). In addition, cold/lower-salinity ice-melt water (IMW; <2.0 °C and <30.0) originates from sea ice, and colder/high-

salinity dense water (DW; less than −1.0 °C and 32.0–33.0) forms in the previous winter during freezing of both the Bering and Chukchi Seas (Weingartner et al., 2013). These water masses often show vertical consistency both geographically and seasonally (Iken et al., 2010; Eisner et al., 2013; Weingartner et al., 2013).

In the northern Bering and Chukchi Seas, copepods are primary consumers of phytoplankton and are the main prey of foraging fish (e.g., polar cod *Boreogadus saida*; Nakano et al., 2015), seabirds (e.g., phalaropes, shearwaters and crested auklets *Aethia cristatella*; Piatt and Springer, 2003; Hunt et al., 2013), and baleen whales (e.g., bowhead whale *Balaena mysticetus*; Lowry et al., 2004). Therefore, copepods are a key component of the Arctic marine food webs (Lowry et al., 2004). In this region, large Arctic copepods (*Calanus glacialis*) and small Arctic copepods (e.g., *Acartia hudsonica*, *Centropages abdominalis*, *Eurytemora herdmani* and *Pseudocalanus acuspes*) are abundant (Springer et al., 1996). In addition, Pacific copepods (*C. marshallae*, *Eucalanus bungii*, *Metridia pacifica*, *Neocalanus cristatus*, *N. flemingeri*, and *N. plumchrus*) are often transported from the Bering Sea (Lane et al., 2008; Hopcroft et al., 2010). Copepod communities are associated with the distribution of water masses (e.g., Springer et al., 1989; Hopcroft et al., 2010; Eisner et al., 2013): *Pseudocalanus* species are abundant in the ACW and Pacific species are abundant in the AW, as they are transported from the Bering Sea. Pacific copepod species (e.g., *E. bungii*) expanded their distribution into the Chukchi Sea in 2007 (Matsuno et al., 2011). *C. glacialis* is abundant in Arctic waters, and it is considered to be a native species to the Arctic shelves (Canover and Huntley, 1991; Ashjian et al., 2003). Therefore, the distribution of copepod communities in this region appears to be affected by both the inflow of Pacific water and the water from sea ice melting.

The distribution patterns of both Pacific and Arctic copepods in the Arctic seas have been reported in these previous studies. However, recent and future drastic climate changes potentially trigger the shifts in the distributions of copepod species or change of their habitat. This phenomenon has already been reported for some species (e.g., Eisner et al., 2014; Ershova et al., 2015). In order to comprehend the response of each copepod group to the environmental changes in the Arctic, a statistical understanding of the relationship between environmental factors and the group's abundance is required. Since Pacific and Arctic copepods have different life cycles, suitable habitat, and reproductive characteristics, their response to the environmental changes are expected to differ. Therefore in the present study, we aim to construct an adequate model to illustrate the suitable environmental

characteristics for each Pacific and Arctic copepods group that will help us predict the risks they might face in the future. Here, we propose the use of generalized additive models (GAMs) to determine the factors affecting the spatial pattern of copepod abundances based on the data collected by net-sampling during the summers of 2007, 2008, and 2013.

2 Materials and methods

2.1 Field sampling

We sampled copepods and water onboard of T/S *Oshoro-maru* (Hokkaido University) during 30 July–24 August 2007 (31 stations), 30 June–13 July 2008 (26 stations), and 4–17 July 2013 (31 stations; Fig. 1). Zooplankton samples were collected during the day or at night using vertical tows with a North Pacific Standard (NORPAC) net (mouth diameter 45 cm, mesh size 335 μm) from 5 m above the bottom to the surface (the depths of most stations were approximately 50 m). The volume of water filtered through the net was estimated using a flow-meter mounted on the mouth of the net. Zooplankton samples were immediately preserved with 5 % v/v borax-buffered formalin. In a laboratory on land, identification and enumeration of taxa were performed on the zooplankton samples under a stereomicroscope. For the dominant taxa (calanoid copepods), identification was made at the species level. In addition to calanoid copepods, cyclopoid copepods such as *Oithona similis* also widely appear in this study area (Llinás et al., 2009). However, we summarized all species as cyclopoid copepods, because we did not perform their identifications at the species level. The species were separated into Pacific and Arctic species based on their dominant reproducing grounds. The applied definition of size (small or large) did not depend on the actual body length of the copepod specimen, but on the generation length and the number of times of reproduction. Falk-Petersen et al. (2009) and Dvoretsky and Dvoretsky (2009) listed the copepod characteristic of distribution, generation length and reproduction. The life cycles of large Arctic copepods includes one or fewer generations per year, whereas small Arctic copepods have multiple generations in the Arctic (e.g., Dvoretsky and Dvoretsky, 2009; Falk-Petersen et al., 2009). Following these two sources, we summarized the copepod species into three groups (Table 2): large Arctic ($CopL_{arc}$: reproducible in the Arctic, and generation length is greater than one year, and reproduction occurs once), small Arctic ($CopS_{arc}$: reproducible in Arctic, generation length less than one year, and reproduction occurs multiple times a year), and Pacific copepods (Cop_{pac}: not reproducible in the Arctic, generation length is greater than one year, and reproduction occurs once).

At the zooplankton sampling stations, vertical profiles of temperature and salinity were made using conductivity-temperature-depth (CTD: Sea-Bird Electronics Inc., SBE 911 Plus) casts. Water samples for chlorophyll *a* were obtained with Niskin bottles on the CTD rosette from the bottom (21–56 m) to the surface. Water samples were gently filtered (<100 mmHg) onto GF/F filters. Phytoplankton pigments on the filters were extracted with *N*,*N*-dimethylformamide (Suzuki and Ishimaru, 1990), and chlorophyll *a* concentrations were determined by the fluorometric method using a Turner Designs 10-AU fluorometer (Welschmeyer, 1994). In order to investigate the relationships between the abundance of copepods and the sea ice condition, we used SSM/I Daily Polar Gridded Sea Ice Concentration (SIC) data obtained from the National Snow and Ice Data Center (http://nsidc.org/).

2.2 Data analysis

The relationship between the abundance of copepods and traditionally defined water masses has been reported (Hopcroft and Kosobokova, 2010; Eisner et al., 2013). In these studies, the surface and bottom water masses were identified based on the basis of temperature and salinity. However, the quantitative evaluation of the effects of complex water properties on the copepod abundance is difficult. In order to quantify the factors affecting the spatial pattern of abundance of each copepod group using GAMs (See Section 2.3), explanatory variables that are correlated with other variables must be removed to avoid the problem of multicollinearity. This procedure may hinder the recovery of important oceanographic features such as the combination of water masses in the upper and bottom layers, because water temperature and salinity in both layers are often strongly correlated. In this study, to delineate the combination of water masses in the upper and bottom layers, we summarized the water-mass properties in these layers as scores using principal component analysis (PCA). These scores can be used as continuous explanatory variables in GAMs.

As the vertical structure of the water mass in our focused region basically forms a one- or two-layered structure because of the shallow bathymetry, we can divide the water column into a maximum of two layers (i.e., the layers above and below the pycnocline are defined as the upper and bottom layers, respectively). The density (ρ) was calculated from the temperature and the salinity measured by CTD profiles with a vertical data resolution of 1 m. We calculated the vertical density gradient ($\frac{d\rho}{dD}$) at a specific depth using 2 m-mean densities

immediately above and below the specific depth. $\frac{d\rho}{dD}$ was calculated for all depths except for the two uppermost and the two lowermost depth levels. The depth of the maximum density gradient ($\frac{d\rho}{dD_{max}}$) was defined as the pycnocline of each sampled site. Then environmental variables (temperature, salinity, and log-transformed chlorophyll *a*) were vertically averaged within the upper and bottom layers and defined as T_{UPP}, T_{BOT}, S_{UPP}, S_{BOT}, Chl.a_{UPP} and Chl.a_{BOT}, respectively (see Table 3 and Figures A1–A4 in Supplementary Materials). PCA was applied to determine the water-mass structure using $\frac{\mathrm{d}\rho}{\mathrm{dD_{max}}}$, T_{UPP}, T_{BOT}, S_{UPP} and S_{BOT} at all 88 stations. As the principal water masses in the Bering and Chukchi Seas are characterized by the temperature and salinity of the water column (Coachman et al., 1975), Chl.a_{UPP}, Chl.a_{BOT} and SIC were not used in the PCA to determine the water-mass structure. These five parameters ($\frac{\mathrm{d}\rho}{\mathrm{dD_{max}}}$, T_{UPP}, T_{BOT}, S_{UPP} and S_{BOT}) were standardized prior to the PCA to reduce the biases between the units of the variables. Several principal components and their factor loadings (correlations of factors to the derived principal components) were presented. The PCA scores were used as covariates of the water-mass structures in the habitat models. In addition, we used the anomaly of timing of sea ice retreat (aTSR) at each sampling station as an index of sea ice condition. The values of aTSR were calculated using satellite-derived sea ice images for 1991–2013. Although sea ice concentration images had been projected using polar stereographic coordinates with 25km spatial resolution, we interpolated them using the nearest-neighbor method and resampled them into 9km spatial resolution. Considering the missing values and land contamination, we defined SIC <50 % as non-ice-covered pixels, and aTSR was defined as the anomalous last date when the SIC fell below 50 % prior to the date of the annual sea ice minimum in the Arctic Ocean.

2.3 Statistical analysis

Before producing the habitat models, we examined the multicollinearity between the explanatory variables by correlation analysis. To examine the relationships between the copepod abundance ($CopL_{arc}$, $CopS_{arc,}$ and Cop_{pac}) and the environmental variables, we constructed habitat models using GAMs. GAMs are a non-parametric extension of generalized linear models (GLMs) such as multiple-regression models (Eq. (1)), with the only underlying assumption that the functions are additive and that the components are smooth (Eq. (2)). The basic concept is the replacement of the parametric GLM structure:

$$g(\mu) = \alpha + \beta_1 x_1 + \beta_2 x_2 + \beta_3 x_3 + \cdots + \beta_i x_i \quad (1)$$

with the additive smoothing function structure:

$$g(\mu) = \varepsilon + s_1(x_1) + s_2(x_2) + s_3(x_3) + \cdots + s_i(x_i) \quad (2)$$

where α and ε are the intercepts and β_i and s_i are the coefficients and the smooth functions of the covariates, respectively (Wood, 2006). To select the most adequate model in our approach, we used Akaike's Information Criterion. Model validation was applied to the optimal models to verify our assumptions and reproducibility of the results. Specifically, we plotted the original values versus the fitted values and judged the adequacy of our optimal models based on R^2. The deviance explained (Eq. (3)) indicates the percentage of the variance that can be explained by the most adequate model, and it is calculated as follows:

$$\text{Deviance explained (\%)} = (1 - \text{Residual Deviance/Null Deviance}) \times 100 \quad (3)$$

where the residual deviance denotes the deviance produced by the model that includes explanatory variables and the null deviance is the deviance produced by the model without explanatory variables. All statistical analyses were undertaken using R (version 2.15.0 http://www.r-project.org).

3 Results

3.1 Principal component analysis and water mass

The first principal component (PC1) explained 47.1 % of the total variability. In the PC1 score, the loading coefficient was positive for $\frac{d\rho}{dD}_{\max}$, indicating that the magnitude of stratification increased with an increase in PC1. In contrast, PC1 was strongly negative for T_{UPP} and T_{BOT}, indicating that lower temperatures in the whole water mass resulted in smaller PC1 (Table 4). Additionally, PC1 was negative for S_{UPP}, indicating a low-salinity water mass in the surface layer with higher PC1, but weakly positive for S_{BOT}. According to Fig. 2a, which shows the T-S diagram colored according to the PC1 score, a higher PC1 value (>1) value indicated a combination of the cold/lower salinity IMW, in the upper layer, and the colder/high-salinity DW, in the bottom layer. In contrast, a low PC1 value denoted a warm water mass in both layers and/or low-salinity surface water (Table 4). From Fig. 2a, a lower PC1 value (<−1.5) indicated a combination of warmer/low-salinity ACW, in the upper layer,

and warm/saline BSW or cold/higher-salinity AW or BSAW, in the bottom layer. A low–medium PC1 score (−1.5–0.5) indicated a combined water mass with both BSW and AW/BSAW (Fig. 2a). PC1 was higher at the stations north of 69°N as compared to ones to the south in 2008 and 2013 and low for all stations in 2007 (Fig. 3), suggesting that the combination of IMW and DW was dominant in the northern stations in 2008 and 2013, and ACW was dominant at almost all stations in 2007.

The second principal component (PC2) explained 34.8 % of the total variability. In the PC2 score, the loading coefficient was negative for $\frac{d\rho}{dD_{max}}$ and temperature and positive for salinity in both the upper and bottom layers (Table 4). These results indicated that there is highly saline water in both layers that tended to decrease the magnitude of stratification and form a single layered structure with higher PC2. As illustrated in Fig. 2b, medium–high PC2 values (>0.5) indicated waters with a single-layered structure, BSW, AW, or BSAW. Low–medium PC2 value (<0.5) denoted waters with a two-layered structure, with warmer-temperature and lower-salinity water in the upper layer compared to the bottom layer, possibly IMW in the upper layer and DW in the bottom layer, or ACW in the upper layer and BSW/AW/BSAW in the bottom layer. PC2 was high at stations <69°N in all years and low at stations east of the survey area in 2007 (Fig. 4), implying that a single-layered structure with BSW/AW/BSAW was dominant in the Bering Strait. However, a combination of ACW with BSW/AW/BSAW was observed northeast of the survey area in 2007.

The third principal component (PC3) explained 14.2 % of the total variability. The PC3 score was correlated positively with all physical variables (Table 4), especially with T_{UPP} and S_{BOT}. According to the T-S diagram colored according to the PC3 values (Fig. 2c), relatively high PC3 values (>0.5) with relatively warm T_{UPP} (>4.0°C) and/or high S_{BOT} (>32.0) suggested that the water columns were composed of ACW in the upper layer and/or high-salinity BSW/AW at the bottom. PC3 was higher in 2007 than in 2008 and 2013, particularly at the stations in the north of the Bering Strait (Fig. 3), indicating that relatively warm BSW/ACW made up the upper layer and/or higher salinity AW/ BSAW/DW the bottom layer.

3.2 Copepod abundance

The recorded abundance of copepods at each station ranged between 150 and 146,323 inds. m^{-2} (median: 14,488). $CopL_{arc}$ included only *Calanus glacialis* (Table 2), which represented

0.00 %–48.2 % of the total abundance and was found over almost the entire study area. $CopL_{arc}$ were more abundant in 2013 than in 2007 and 2008 (Fig. 4). $CopS_{arc}$ made up 1.47 %–55.6 % of the total copepod abundance at each station and included *Pseudocalanus* spp, *P. minutus*, *P. mimus*, *P. newmani*, and *P. acuspes* (Table 2). $CopS_{arc}$ were dominant throughout the study area in all study seasons (Fig. 4). Cop_{pac} included *C. marshallae*, *N. cristatus*, *N. flemingeri*, *N. plumchrus*, *E. bungii*, and *M. pacifica*. Cop_{pac} were more abundant in the south (<69°N) than in the north during all studied time intervals (Fig. 4).

3.3 Copepod habitats

We constructed habitat models using aTSR, the quantitative index of the water masses (PC1, PC2, and PC3), bottom depth (Bdepth), and averaged log-transformed chlorophyll *a* in the upper layer (Chl.a_{UPP}) and in the bottom layer (Chl.a_{BOT}) as potential explanatory variables. Averaged physical factors in the upper layer and bottom layers were excluded from potential explanatory variables, as these were already included in the quantitative index of the water masses.

The model most adequately explaining the abundance of $CopL_{arc}$ included all explanatory variables (Table 5). $CopL_{arc}$ were abundant at stations with lower aTSR (<0 days) and with deeper Bdepth, especially in the areas with bottom depths greater than 45 m (Fig. 5). $CopL_{arc}$ appeared to be abundant at stations with medium–higher PC1 (> −0.5), low–high PC2 (−1 to 1), and low–medium PC3 (−1 to 0). The abundance of $CopL_{arc}$ was relatively high in waters with low (less than −0.5) and high (0.2–0.5) Chl.a_{UPP}. However, the effects of Chl.a_{UPP} and Chl.a_{BOT} on $CopL_{arc}$ were not clear.

The model which explains the abundance of $CopS_{arc}$ most adequately, included all explanatory variables except PC2 (Table 5). $CopS_{arc}$ were abundant at stations with lower aTSR (< 5days) and with deeper Bdepth, especially in the areas where the sea depth was greater than 40 m (Fig. 5). The abundance of $CopS_{arc}$ was high for low–high PC1 (between −1.5 and 2) and medium PC3 (0–1.2), and for medium–high Chl.a_{UPP} (>0; Fig. 5). The effect of Chl.a_{BOT} was unclear.

The abundance of Cop_{pac} was most adequately explained by the model with all explanatory variables except Chl.a_{UPP} (Table 5). Cop_{pac} were abundant at stations with low aTSR (<0 days), deeper Bdepth with a clear positive effect in waters deeper than 35 m, low–medium PC1 (−2 to 0.5) and PC3 (−0.5 to 1) and PC2 (< −0.5); it is less abundant at stations

with medium–high PC2 (> −0.5) and high PC1 (>0.5; Fig. 5). The abundance of Cop_{pac} was high in the waters with low (< −0.2) and high (>0.5) Chl.a_{BOT}; however, the effect of Chl.a_{BOT} on Cop_{pac} was not clear.

4 Discussion

4.1 Effect of sea ice on copepod abundance

The models most adequate to explain the abundance of copepods included aTSR as an explanatory variable (Table 5). As shown in the GAM plot, earlier sea ice retreat had positive effects on the abundance of all copepod groups (Fig. 5); in particular, the effect of early sea ice retreat was more obvious for Cop_{arc} than for the other two groups. The Cop_{pac} typified by *C. marshallae* and *N. cristatus*, are often transported from the Bering Sea through the Bering Strait (Lane et al., 2008; Hopcroft et al., 2010; Matsuno et al., 2011). Sea ice reduction is strongly related to an increase in the inflow of Pacific water from the Bering Sea through the Bering Strait (Shimada et al., 2006). Increasing water-mass transportation into the Chukchi Sea (Woodgate et al., 2012) and sea ice retreat enhances the northward invasion by larger Pacific water species. Our results reflect that future increases in advection from the Bering Sea will carry more Pacific zooplankton through the Bering Strait with even further penetration into the Arctic.

Temperature and food are important for the growth of $CopL_{arc}$ and $CopS_{arc}$ that reproduce in the Arctic. There is a strong relationship between the mean developmental stage (Copepodite stage I–V) of *C. glacialis* and surface temperature (Ershova et al., 2015). Early sea ice retreat leads to a longer ice-free period and warmer surface temperature. In our study, aTSR is negatively correlated with T_{UPP} and T_{BOT} (ρ = −0.59 and −0.69, respectively; Spearman's correlation test $p < 0.001$), i.e., the sampling stations with early sea ice retreat have relatively high temperature and favorable conditions for copepod growth. The spring bloom inevitably forms at the ice edge and its timing is controlled by the timing of the sea ice retreat in the northern Bering Sea (Brown and Arrigo, 2013). In the shelf regions of the Bering and Chukchi Seas, early sea ice retreat leads to spring blooms in open water (Fujiwara et al., 2016). For copepods, the spring bloom resulting from early sea ice retreat is an important energy source, because a large supply of food can be utilized while maintaining high activity in relatively warm ice-free waters or even cold, when close to the melt period.

Thus, earlier sea ice retreat should have positive effects on the growth and reproduction of copepods that do not rely on sea ice production in the northern Bering and Chukchi Seas.

4.2 Effects of water mass on copepod abundance

The abundance of all copepods was variably related to the combination of water masses in the northern Bering and Chukchi Seas. In these seas, it has been well documented that the community structure and abundance of zooplankton species differ in the different water masses (e.g., Lane et al., 2008; Hopcroft et al., 2010; Matsuno et al., 2011), including the six major water masses; ACW, IMW, DW, BSW, AW, and BSAW (e.g., Coachman et al., 1975; Springer et al., 1989). These water masses and their combinations have mostly been described by cluster analysis using temperature and salinity (e.g., Norcross et al., 2010; Eisner et al., 2013; Ershova et al., 2015). In the present study, we quantitatively characterized these water masses using PCA incorporating the combined water masses, the number of layers (single- or double-layered masses), and the occurrence of high-salinity water in the bottom layer and/or warm water in the upper layer (Fig. 2).

$CopL_{arc}$ were relatively abundant in the northern part of the Chukchi Sea (>69°N), which is dominated by the cold/lower-salinity IMW water mass in the upper layer and the colder/high-salinity DW in the bottom layer (PC1 > 1, −1 < PC2 < −0.8, and −1 < PC3 < 0; Figs. 3, 4). This combination of water masses is positively correlated with the abundance of $CopL_{arc}$ (Fig. 5), represented solely by *Calanus glacialis* in the study area. This species is considered to be native to Arctic shelves (Conover and Huntley, 1991; Ashjian et al. 2003). The Arctic population of *C. glacialis* appears in winter water in the study area (Ershova et al., 2015). Our results back these $CopL_{arc}$ habitats. Previous findings have reported that *C. glacialis* were also abundant in water masses with ACW in the upper layer and BSAW in the bottom layer (Eisner et al., 2013). In the present study, $CopL_{arc}$ were relatively abundant in the Bering Strait, in areas dominated by cold/high to higher-salinity BSAW and AW in both layers (−1.5 < PC1 <1, −0.8 < PC2 <1.2, and PC3 < −1) in 2013. However, $CopL_{arc}$ in this study are less abundant in the water off Point Hope (southern part of the Chukchi Sea); this area was characterized by ACW in the upper layer and BSAW in the bottom layer (−2.5 < PC1 < −1.5 and PC3 >0; Fig. 5) during the summer of 2007. Our results slightly contradict those of the above previous study; however, the presence of BSAW/AW is important for $CopL_{arc}$.

In contrast to $CopL_{arc}$, $CopS_{arc}$ were common in the entire study area. This copepod group was abundant in waters with medium PC1 and PC3, indicating that these taxa were distributed in waters with a wide range of temperature and salinity, i.e., warm/saline BSW. However, $CopS_{arc}$ were less abundant in waters with higher PC1, i.e., colder/low-salinity IMW in the upper layer and cold/high-salinity DW in the bottom layer. These support the previous findings that small Arctic copepods (e.g., *Pseudocalanus* spp., *A. hudsonica* and *A. longiremis*) were abundant in warm BSW and relatively warm ACW in the upper and/or bottom layers (Eisner et al., 2013; Ershova et al., 2015). In this study, $CopS_{arc}$ were dominated by *Pseudocalanus*, including *Pseudocalanus acuspes*, *P. mimus*, *P. minutus*, *P. newmani*, and undefined *Pseudocalanus* spp. (mean 72 % of $CopS_{arc}$ abundance). *Pseudocalanus* occurs in the entire of Bering Sea shelf and in the Arctic area (Frost, 1989). This distribution is thought to result from *Pseudocalanus* being initially abundant in the warm water originating from the Bering Sea. According to Questel et al., (2016), *P. mimus* and *P. newmani*, summarized into $CopS_{arc}$ in our study, are considered more Pacific by origin. Arctic/Pacific species are identified as such based on whether or not they are reproducible in Arctic region; thus, *P. mimus* and *P. newmani* are identified as $CopS_{arc}$. Unfortunately, we did not analyze the genetic type of copepods individually, so we could not determine their origins. However, *P. mimus* and *P. newmani* might be transported to the Arctic by the Pacific inflow. Therefore $CopS_{arc}$ are significantly abundant in the warm-water masses such as ACW and BSW. The abundance of $CopL_{arc}$ could be associated with cold-water masses in which $CopS_{arc}$ are less abundant.

Pacific zooplankton are advected into the western Arctic Ocean through the Bering Strait (Springer et al., 1989). Previous studies demonstrated that Pacific zooplankton communities occurred in high-salinity water (BSW/AW) in the northern Bering and Chukchi Seas (Springer et al., 1989; Lane et al., 2008; Hopcroft et al., 2010; Matsuno et al., 2011; Eisner et al., 2013). In this study, Pacific copepods (Cop_{pac}) were abundant in the Bering Strait and the Chukchi Sea south of Point Hope, areas which have low–medium PC1 and PC2, associated with warmer/low-salinity ACW in the upper layer and cold/higher-salinity AW and warm/saline BSW or BSAW in the bottom layer, or single-layered AW, BSW, and BSAW. These results support the previous observations. Our study further confirms the effects of the interannual water-mass variability on copepod abundance. During the summer of 2007, Pacific water masses (ACW, BSW and BSAW) extended to the north of 69°N (Fig. 3) and transported Cop_{pac} into the Chukchi Sea (Matsuno et al., 2011). In contrast, in the summers of

2008 and 2013, when IMW and colder/high-salinity DW were dominant, few Cop_{pac} were collected in the northern part of the Chukchi Sea (Fig. 4).

The combinations and distributions of water masses are known to be affected by the Pacific inflow (Weingartner et al., 2005) and related to the sea ice retreat (Coachman et al., 1975; Day et al., 2010). The inflow of warmer Pacific ACW was dominant in 2007 (Woodgate et al., 2010), and this strong inflow is believed to have triggered the sea ice retreat in the western Arctic Ocean (Woodgate et al., 2012). Thus, the variability of the water masses and their combinations as illustrated by PCA were in good agreement with the conventional description of the dynamics of water masses. Our index can be used for the quantitative evaluation of the effects of water-mass combinations with multiple components of water properties and so may be useful for predicting copepod distributions with climate changes.

4.3 Effects of phytoplankton and bottom depth

The species categorized as $CopS_{arc}$ (e.g., *Pseudocalanus* spp.) graze phytoplankton and reproduce in the surface layer during day and night in the summer (Norrbin et al., 1996; Plourde et al., 2002; Harvey et al., 2009). We therefore expected positive effects of Chl.a_{UPP} on the $CopS_{arc}$ abundance. However, the models did not yield obvious relationships between the abundance of any copepods and Chl.a_{UPP}. Besides, there is possibility that young copepodite stages could not be sampled with a coarse net (> 300 μm) such as the NORPAC net used for our sampling. Moreover, another plausible explanation is that the sampling period (June–August) did not coincide with the high-grazing and reproduction season when copepods require a large amount of food intake. $CopL_{arc}$ reproduce during the spring phytoplankton bloom (e.g., Falk-Petersen et al., 2009); thus our sampling period was not the time of their reproduction. Phytoplankton cells sinking to the bottom water layers are important food for copepods (Sameoto et al., 1986). Consequently, we also expected a positive effect of the bottom chlorophyll *a* concentration (Chl.a_{BOT}) on the abundance of all copepod groups. However, clear positive effects were not observed (Fig. 5). In addition, another important explanation for the non-correlation between phyto- and zooplankton values is the different temporal scales in population growth. A relationship may have been shown using the cumulative phytoplankton production from the ice break-up to the sampling time, which is difficult to obtain. Therefore, it is difficult to link the chlorophyll *a* concentration to the copepod abundance using the time lag between the blooms of phytoplankton and copepods.

A few previous studies have reported associations between the copepod abundance and the bottom depth of the shelf in the northern Bering and Chukchi Seas (e.g., Ashjian et al., 2003). The reason for copepod groups being less abundant in waters shallower than 32 m bottom depth was unclear. In this survey, because the shallower area is correlated with the longitude ($\rho = -0.73$; Spearman's rank correlation test of longitude (°E) vs. Bdepth, $p < 0.001$), the result indicates that copepods are less abundant near the land. As shown in Figure 5, the smallest number of copepods was recorded at sampling stations of 25 m Bdepth. Except for these two stations, $CopL_{arc}$ are not obviously related to Bdepth, whereas Cop_{pac} and $CopS_{arc}$ gradually increase with depth.

The associations between environmental factors and the abundance of copepods have been well documented (e.g., Springer et al., 1989; Lane et al., 2008; Matsuno et al., 2011). Recently these relationships were analyzed using clustered water masses (Eisner et al., 2013; Ershova et al., 2015). In the present study, we indexed the water masses and then quantitatively modeled the relationships between the water-mass characteristics and the spatial patterns of copepod abundance. Our evaluation of the effect of changes in the timing of sea ice retreat on copepod abundance confirms that suitable environments for copepods are formed by early sea ice retreat. The influence of the changes in sea ice on the Arctic ecosystem has been already documented; however, to the best of our knowledge, this is the first quantitative study to describe the relationships between the early sea ice retreat and copepod abundance. Quantitative analyses using the habitat models are useful for understanding various phenomena and risks faced by organisms (e.g., sea ice loss, temperature increase, and enhanced sea water freshening). Furthermore, this type of analysis can be adapted to predict ecosystem changes in the future by incorporating climate and predicted environmental data, and can also be used to understand the responses of organisms to environmental change in the northern Bering and Chukchi Seas.

Author contributions

T.K. designed and coordinated this research project. K.M. and A.Y. collected the zooplankton samples, performed species identification and enumeration of the zooplankton samples in the land laboratory. A.F. operated and calculated sea-ice concentration data. H.U. and M.O. calculated the stratification index by using CTD profiles. H.S. and Y.W. wrote the manuscript with contributions from all co-authors.

Acknowledgements

We would like to acknowledge the Captain, crew, and all students on-board during the T/S *Oshoro-Maru* on the summer of 2007, 2008, and 2013 cruises for their endless support and hard work. And we thank Hisatomo Waga and all students who collected the water samples and measured chlorophyll-*a* concentration. We also thank the member of laboratory of marine ecology in Hokkaido University. This study was supported by the Green Network of Excellence Program's (GRENE Program) Arctic Climate Change Research Project : 'Rapid Change of the Arctic Climate System and its Global Influences'.

References

Arrigo, K. R., van Dijken, G., and Pabi, S.: Impact of a shrinking Arctic ice cover on marine primary production, Geophys. Res. Lett., 35, L19603, 2008.

Ashjian, C. J., Campbell, R. G., Welch, H. E., Butler, M., and Van Keuren, D.: Annual cycle in abundance, distribution, and size in relation to hydrography of important copepod species in the western Arctic Ocean, Deep-Sea Res. Pt. I, 50, 1235-1261, 2003.

Brown, Z. W., and Arrigo, K. R.: Sea ice impacts on spring bloom dynamics and net primary production in the Eastern Bering Sea, J. Geophys. Res.-Oceans, 118, 43-62, 2013.

Clement, J. L., Cooper, L. W., and Grebmeier, J. M.: Late winter water column and sea ice conditions in the northern Bering Sea, J. Geophys. Res.-Oceans, 109, 2004.

Coachman, L. K., Aagaard, K., and Tripp, R. B.: Bering Strait: the regional physical oceanography, University of Washington Press, 1975.

Coachman, L. K.: Advection and mixing on the Bering Chukchi Shelves. Component A. Advection and mixing of coastal water on high latitude shelves, ISHTAR 1986 Progress Report, Vol. I., Inst. Mar. Sci. Univ. Alaska, Fairbanks, 1987.

Comiso, J. C., Parkinson, C. L., Gersten, R., and Stock, L.: Accelerated decline in the Arctic sea ice cover, Geophys. Res. Lett., 35, L01703, 2008.

Conover, R. J., and M. Huntley, M.: Copepods in ice-covered seas—distribution, adaptations to seasonally limited food, metabolism, growth patterns and life cycle strategies in polar seas, J. Mar. Syst., 2-1, 1-41, 1991.

Day, R. H., Weingartner, T. J., Hopcroft, R. R., Aerts, L. A. M., Blanchard, A. L., Gall, A. E., Gallaway, B. J., Hannay, D. E., Holladay, B. A., Mathis, J. T., Norcross, B. L., Questel, J. M., and Wisdom, S. S.: The offshore northeastern Chukchi Sea, Alaska: A complex high-latitude ecosystem, Cont. Shelf Res., 67, 147-165, 2013.

Dvoretsky, V., and Dvoretsky, A.: Life cycle of *Oithona similis* (Copepoda: Cyclopoida) in Kola Bay (Barents Sea), Mar. Biol., 156, 1433-1446, 2009.

Eisner, L., Hillgruber, N., Martinson, E., and Maselko, J.: Pelagic fish and zooplankton species assemblages in relation to water mass characteristics in the northern Bering and southeast Chukchi seas, Polar Biol., 36, 87-113, 2013.

Ershova, E. A., Hopcroft, R. R., and Kosobokova, K. N.: Inter-annual variability of summer mesozooplankton communities of the western Chukchi Sea: 2004–2012, Polar Biol., 38, 1461-1481, 2015.

Falk-Petersen, S., Mayzaud, P., Kattner, G., and Sargent, J. R.: Lipids and life strategy of Arctic *Calanus*, Mar. Biol. Res., 5, 18-39, 2009.

Feder, H. M., Foster, N. R., Jewett, S. C., Weingartner, T. J., and Baxter, R.: Mollusks in the northeastern Chukchi Sea. Arctic, 145-163, 1994.

Frost, B. W.: A taxonomy of marine clanoid copepod genus Pseudocalanus, Can. J. Zool., 67, 525–551, 1989.

Fujiwara, A., Hirawake, T., Suzuki, K., Eisner, L., Imai, I., Nishino, S., Kikuchi, T., and Saitoh, S. I.: Influence of timing of sea ice retreat on phytoplankton size during marginal ice zone bloom period on the Chukchi and Bering shelves, Biogeosciences, 13(1), 115-131, 2016.

Grebmeier, J. M., McRoy, C. P., and Feder, H. M.: Pelagic-benthic coupling on the shelf of the northern Bering and Chukchi Seas. I. Food supply source and benthic biomass, Mar Ecol. Prog. Ser, 48, 57-67, 1988.

Grebmeier, J. M., Feder, H. M., and McRoy, C. P.: Pelagic-benthic coupling on the shelf of the northern Bering and Chukchi Seas. 11. Benthic community structure. Mar. Ecol. Prog. Ser, 51, 253-268, 1989.

Grebmeier, J. M., Overland, J. E., Moore, S. E., Farley, E. V., Carmack, E. C., Cooper, L. W., Frey, K. E., Helle, J. H., McLaughlin, F. A., and McNutt, S. L.: A major ecosystem shift in the northern Bering Sea, Science, 311, 1461-1464, 2006.

Grebmeier, J. M., Moore, S. E., Overland, J. E., Frey, K. E., and Gradinger, R.: Biological response to recent Pacific Arctic sea ice retreats, Eos, Transactions American Geophysical Union, 91, 161-162, 2010.

Grebmeier, J. M., Bluhm, B. A., Cooper, L. W., Danielson, S. L., Arrigo, K. R., Blanchard, A. L., Clarke, J. T., Day, R. D., Frey, K. E., Gradinger, R. R., Kędra, M., Konar, B., Kuletz, K. K., Lee, S. H., Lovvorn, J. R., Norcross, B. L. and Okkonen, S. R.: Ecosystem characteristics and processes facilitating persistent macrobenthic biomass

hotspots and associated benthivory in the Pacific Arctic. Prog. Oceanogr., 136, 92-114, 2015.

Harvey, M., Galbraith, P. S., and Descroix, A.: Vertical distribution and diel migration of macrozooplankton in the St. Lawrence marine system (Canada) in relation with the cold intermediate layer thermal properties, Prog. Oceanogr., 80, 1-21, 2009.

Hopcroft, R. R., and Kosobokova, K. N.: Distribution and egg production of *Pseudocalanus* species in the Chukchi Sea, Deep-Sea Res. Pt. II, 57, 49-56, 2010.

Hopcroft, R. R., Kosobokova, K. N., and Pinchuk, A. I.: Zooplankton community patterns in the Chukchi Sea during summer 2004, Deep-Sea Res. Pt. II, 57, 27-39, 2010.

Hunt, G. L., Blanchard, A. L., Boveng, P., Dalpadado, P., Drinkwater, K. F., Eisner, L., Hopcroft, R. R., Kovacs, K. M., Norcross, B. L., and Renaud, P.: The Barents and Chukchi Seas: comparison of two Arctic shelf ecosystems, J. Mar. Syst., 109, 43-68, 2013.

Iken, K., Bluhm, B., and Dunton, K.: Benthic food-web structure under differing water mass properties in the southern Chukchi Sea, Deep-Sea Res. Pt. II, 57, 71-85, 2010.

Kahru, M., Brotas, V., Manzano-Sarabia, M., and Mitchell, B.G.: Are phytoplankton blooms occurring earlier in the Arctic?, Glob. Change Biol, 17, 1733-1739, 2011.

Lane, P. V. Z., Llinás, L., Smith, S. L., and Pilz, D.: Zooplankton distribution in the western Arctic during summer 2002: Hydrographic habitats and implications for food chain dynamics, J. Mar. Syst., 70, 97-133, 2008.

Llinás, L., Pickart, R. S, Mathis, J. T., and Smith S. L.: Zooplankton inside an Arctic Ocean cold-core eddy: Probable origin and fate, Deep-Sea Res. Pt. II, 56, 1290-1304, 2009.

Lowry, L. F., Sheffield, G., and George, J. C.: Bowhead whale feeding in the Alaskan Beaufort Sea, based on stomach contents analyses, J. Cetacean Res. Manage., 6, 215-223, 2004.

Matsuno, K., Yamaguchi, A., Hirawake, T., and Imai, I.: Year-to-year changes of the mesozooplankton community in the Chukchi Sea during summers of 1991, 1992 and 2007, 2008, Polar Biol., 34, 1349-1360, 2011.

Matsuno, K., Yamaguchi, A., Hirawake, T., Nishino, S., Inoue, J., and Kikuchi, T.: Reproductive success of Pacific copepods in the Arctic Ocean and the possibility of

changes in the Arctic ecosystem, Polar Biol., 1-5, doi:10.1007/s00300-015-1658-3, 2015.

Nakano, T., Matsuno, K., Nishizawa, B., Iwahara, Y., Mitani, Y., Yamamoto, J., Sakurai, Y., and Watanuki, Y.: Diets and body condition of polar cod (*Boreogadus saida*) in the northern Bering Sea and Chukchi Sea, Polar Biol., 1-6, 2015.

Norcross, B. L., Holladay, B. A., Busby, M. S., and Mier, K. L.: Demersal and larval fish assemblages in the Chukchi Sea, Deep-Sea Res Pt. II, 57, 57-70, 2010.

Norrbin, M., Davis, C., and Gallager, S.: Differences in fine-scale structure and composition of zooplankton between mixed and stratified regions of Georges Bank, Deep-Sea Res Pt. II, 43, 1905-1924, 1996.

Parkinson, C. L., and Comiso, J. C.: On the 2012 record low Arctic sea ice cover: Combined impact of preconditioning and an August storm, Geophys. Res. Lett., 40.7, 1356-1361, doi: 10.1002/grl.50349, 2013.

Piatt, J. F., and Springer, A. M.: Advection, pelagic food webs and the biogeography of seabirds in Beringia, Mar. Ornith., 31, 141-154, 2003.

Plourde, S., Dodson, J. J., Runge, J. A., and Therriault, J. C.: Spatial and temporal variations in copepod community structure in the lower St. Lawrence Estuary, Canada, Mar. Ecol.-Prog. Ser., 230, 211-224, 2002.

Questel, J.M., Blanco-Bercial, L., Hopcroft, R.R., Bucklin, A.: Phylogeography and connectivity of the *Pseudocalanus* (Copepoda: Calanoida) species complex in the eastern North Pacific and the Pacific Arctic Region, J. Plankton Res., 38, 610-623, 2016.

Sameoto, D., Herman, A., and Longhurst, A.: Relations between the thermocline meso and microzooplankton, chlorophyll a and primary production distributions in Lancaster Sound, Pol. Biol., 6, 53-61, 1986.

Shimada, K., Kamoshida, T., Itoh, M., Nishino, S., Carmack, E., McLaughlin, F., Zimmermann, S., and Proshutinsky, A.: Pacific Ocean inflow: Influence on catastrophic reduction of sea ice cover in the Arctic Ocean, Geophys. Res. Lett., 33.8, L08605, 2006.

Sigler, M. F., Stabeno, P. J., Eisner, L. B., Napp, J. M., and Mueter, F. J.: Spring and fall phytoplankton blooms in a productive subarctic ecosystem, the eastern Bering Sea, during 1995–2011, Deep-Sea Res. Pt. II, 109, 71-83, 2014.

Spall, M. A., Pickart, R. S., Brugler, E. T., Moore, G. W. K., Thomas, L., and Arrigo, K. R.: Role of shelfbreak upwelling in the formation of a massive under-ice bloom in the Chukchi Sea. Deep-Sea Res. Pt. II, 105, 17-29, 2014.

Springer, A. M., McRoy, C. P., and Turco, K. R.: The paradox of pelagic food webs in the northern Bering Sea—II. Zooplankton communities, Cont. Shelf Res., 9, 359-386, 1989.

Springer, A. M., McRoy, C. P., and Flint, M. V.: The Bering Sea Green Belt: Shelf-edge processes and ecosystem production, Fish. Oceanogra., 5, 205-223, 1996.

Stabeno, P., Bond, N., and Salo, S.: On the recent warming of the southeastern Bering Sea shelf, Deep-Sea Res. Pt. II, 54, 2599-2618, 2007.

Suzuki, R., and Ishimaru, T.: An improved method for the determination of phytoplankton chlorophyll using N, N-dimethylformamide, J. Oceanogr. Soci. Japan, 46, 190-194, 1990.

Weingartner, T., Aagaard, K., Woodgate, R., Danielson, S., Sasaki, Y., and Cavalieri, D.: Circulation on the north central Chukchi Sea shelf, Deep-Sea Res. Pt. II, 52, 3150-3174, 2005.

Weingartner, T., Dobbins, E., Danielson, S., Winsor, P., Potter, R., and Statscewich, H.: Hydrographic variability over the northeastern Chukchi Sea shelf in summer-fall 2008–2010, Cont. Shelf Res., 67, 5-22, 2013.

Welschmeyer, N. A.: Fluorometric analysis of chlorophyll *a* in the presence of chlorophyll b and pheopigments, Limnol. Oceanogr., 39, 1985-1992, 1994.

Wood, S. N.: Generalized Additive Models: An introduction with R, CRC Press, 2006.

Woodgate, R. A., Weingartner, T., and Lindsay, R.: The 2007 Bering Strait oceanic heat flux and anomalous Arctic sea‐ice retreat, Geophys. Res. Lett., 37, L01602, 2010.

Woodgate, R. A., Weingartner, T. J., and Lindsay, R.: Observed increases in Bering Strait oceanic fluxes from the Pacific to the Arctic from 2001 to 2011 and their impacts on the Arctic Ocean water column, Geophys. Res. Lett., 39, L24603, 2012.

Figure captions

Figure 1. Study area and sampling stations in the northern Bering and Chukchi Seas during the summers of 2007, 2008 and 2013. The symbols denote the sampling stations where NORPAC net and CTD water samplings were conducted. Modified from figure presented in Spall et al. (2014) and Grebmeier et al. (2015).

Figure 2. T-S diagrams of principal component scores (a) PC1, (b) PC2 and PC3 (c). Colored circle indicated the magnitude of each PC.

Figure 3. Distribution of main principal component score (PC1–3) in 2007, 2008 and 2013. Colored circles indicates magnitude of PC.

Figure 4. Distribution of copepods abundance in 2007, 2008 and 2013. large Arctic ($CopL_{arc}$), small Arctic ($CopS_{arc}$) and Pacific (Cop_{pac}) copepods.

Figure 5. GAM plot of the best model in each copepod groups: large Arctic ($CopL_{arc}$), small Arctic ($CopS_{arc}$) and Pacific (Cop_{pac}) copepods. The horizontal axes show the explanatory variable: the anomaly of the timing of sea-ice retreat (aTSR), principal component score (PC1–3) averaged log-transformed chlorophyll *a* concentration within the layer above and below pycnocline, (Chl a_{UPP} and Chl a_{BOT}) and bottom depth (Bdepth). Shade area represents 95% confidence intervals. The vertical axes indicate the estimate smoother for the abundance of copepods. The estimated smoother converts the explanatory variable to fit the models, so it shows positive effects for response variables and the magnitude of its effects when estimated smoother is positive, and vise versa. Short vertical lines located on the *x* axes of each plot indicate the values at which observations were made.

Supplementary materials

Figure A1. Maximum density gradient (10^{-3} kg m^{-1}) at each sampling station.

Figure A2. Horizontal distributions of temperature (°C) averaged within the upper (T_{UPP}, top panels) and the bottom (T_{BOT}, bottom panels) layers at each sampling station in 2007 (left panels), 2008 (middle panels) and 2013 (right panels).

Figure A3. Same as figure A2 but for salinity (S_{UPP} and S_{BOT}).

Figure A4. Same as figure A2 but for Chlorophyll-*a* concentration (Chla_{UPP} and Chla_{BOT}).

Figure B1. Climatological mean sea ice retreat date of 1991-2013.

1 **Figure B2.** The anomaly of sea ice retreat at all sampling locations in 2007, 2008 and 2013
2 based on daily passive microwave sea ice concentrations using a threshold of 40%.

3 **Figure B3.** Correlation charts of with aTSR thresholds of 50 % vs. 0–40 %.

4

Table 1. Water mass properties in the northern Bering and Chukchi Seas.

Water mass	Temperature	Salinity	Reference
Alaskan coastal water (ACW)	relatively warm (2.0–13.0 °C)	low (< 31.8)	Coachman et al. (1975)
Bering Shelf Water (BSW)	warm (0.0–10.0 °C)	saline (31.8–32.5)	Coachman et al. (1987) Grebmeier et al. (1988) Springer et al. (1989)
Anadyr water (AW)	cold (-1.0–1.5 °C)	high (32.5–33.3)	Coachman et al. (1987) Grebmeier et al. (1988) Springer et al. (1989)
Bering Shelf Anadyr water (BSAW)	cold (-1.0–2.0 °C)	high (31.8–33.0)	Grebmeier et al. (1989) Eisner et al. (2013)
ice melt water (IMW)	cold (< 2.0 °C)	low (< 30.0)	Weingartner et al. (2005)
dense water (DW)	cold (< -1.0 °C)	high (32.0–33.0)	Coachman et al. (1975) Feder et al. (1994)

Table 2. The copepods species included in each copepod groups: large Arctic ($CopL_{arc}$), small Arctic ($CopS_{arc}$) and Pacific (Cop_{pac}) copepods.

Response Variables	Description	Species
$CopL_{arc}$	large Arctic copepods	*Calanus glacialis*
$CopS_{arc}$	small Arctic copepods	*Acartia hudsonica*
		Acartia longiremis
		Acartia tumida
		Centropages abdominalis
		Eurytemora herdmani
		Epilabidocera amphitrites
		Microcalanus pygmaeus
		Pseudocalanus acuspes
		Pseudocalanus mimus
		Pseudocalanus minutus
		Pseudocalanus newmani
		Pseudocalanus spp.
		Scolecithricella minor
		Tortanus discaudatus
		Cyclopoid copepods
Cop_{pac}	Pacific copepods	*Calanus marshallae*
		Eucalanus bungii
		Metridia pacifica
		Neocalanus cristatus
		Neocalanus flemingeri
		Neocalanus plumchrus

Table 3. The covariates for principal component analysis and explanatory variables for Generalize Additive Models (GAMs).

Explanatory variables in GAMs	Environmental Variables	Description	Unit
The principal components (PC1, PC2 and PC3)	$\frac{d\rho}{dD_{max}}$	Magnitude of the maximum potential density gradient	10^{-3} g m^{-1}
	T_{UPP}	Vertical averaged temperature above the depth of the maximum potential density gradient	°C
	T_{BOT}	Vertical averaged temperature under the depth of the maximum potential density gradient	°C
	S_{UPP}	Vertical averaged salinity above the depth of the maximum potential density gradient	
	S_{BOT}	Vertical averaged salinity under the depth of the maximum potential density gradient	
BDepth	Depth	Bottom depth	m
Chl.a_{UPP}	Chl.a_{UPP}	Vertical averaged log-transformed Chlorophyll-*a* concentration above the depth of the maximum potential density gradient	
Chl.a_{BOT}	Chl.a_{BOT}	Vertical averaged log-transformed Chlorophyll-*a* concentration under the depth of the maximum potential density gradient	
aTSR	aTSR	Temporal difference from the Timing of Sea ice Retreat (TSR) anomaly to TSR between 1991 and 2013	days

Table 4. Eigenvalue and factor loadings of principle component analysis. The variances and eigenvalue of each principal component (PC) are also given. Descriptions of elements are same as Table 3 (See Table 3).

Elements	Eigenvector (Factor loadings)									
	PC1		PC2		PC3		PCA4		PCA5	
$\frac{d\rho}{dD_{max}}$	0.36	(0.55)	-0.55	(-0.73)	0.45	(0.38)	-0.27	(-0.10)	0.54	(0.15)
T_{UPP}	-0.51	(-0.78)	-0.38	(-0.50)	0.38	(0.32)	-0.38	(-0.13)	-0.56	(-0.15)
S_{UPP}	-0.43	(-0.66)	0.54	(0.71)	0.11	(0.09)	-0.54	(-0.19)	0.47	(0.13)
T_{BOT}	-0.60	(-0.92)	-0.18	(-0.24)	0.21	(0.18)	0.65	(0.23)	0.37	(0.10)
S_{BOT}	0.27	(0.41)	0.48	(0.63)	0.77	(0.65)	0.24	(0.08)	-0.21	(-0.06)
Eigenvalue	2.66		1.74		0.71		0.12		0.07	
Standard deviation	1.54		1.32		0.84		0.35		0.27	
Proportion of variance (%)	47.13		34.79		14.17		2.43		1.49	
Cumulative proportion (%)	47.13		81.92		96.08		98.51		100.00	

Table 5. Best models of each copepod groups: large Arctic ($CopL_{arc}$), small Arctic ($CopS_{arc}$) and Pacific (Cop_{pac}) copepods.

Response variables	Best models	Deviance Explained (%)	Observed vs. Fitted
			R^2
$CopL_{arc}$	s(aTSR)+s(PC1)+s(PC2)+s(PC3)+s(Chl.a_{UPP})+s(Chl.a_{BOT})+s(Bdepth)+ ε	92.4	0.94
$CopS_{arc}$	s(aTSR)+ s(PC1)+s(PC3)+s(Chl.a_{UPP})+s(Chl.a_{BOT})+s(Bdepth)+ ε	89.9	0.88
Cop_{pac}	s(aTSR)+ s(PC1)+s(PC2)+s(PC3)+s(Chl.a_{BOT})+s(Bdepth)+ ε	75.3	0.38

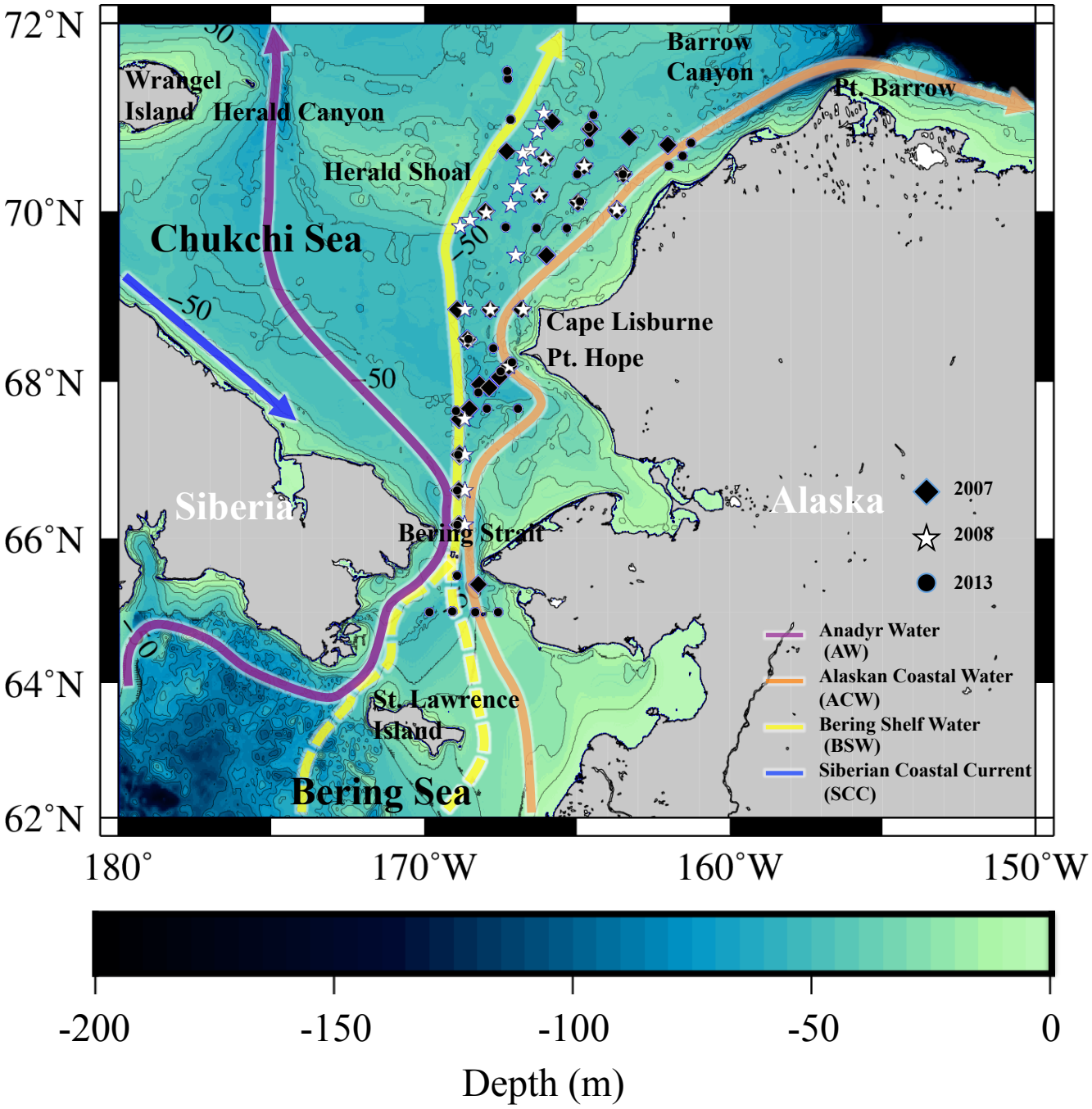
72°N
70°N
68°N
66°N
64°N
62°N
180°
170°W
160°W
150°W
Wrangel Island
Herald Canyon
Herald Shoal
Barrow Canyon
Pt. Barrow
Chukchi Sea
Cape Lisburne
Pt. Hope
Siberia
Alaska
Bering Strait
St. Lawrence Island
Bering Sea
-50
-50
-50
-50
-50
2007
2008
2013
Anadyr Water (AW)
Alaskan Coastal Water (ACW)
Bering Shelf Water (BSW)
Siberian Coastal Current (SCC)
-200
-150
-100
-50
0
Depth (m)

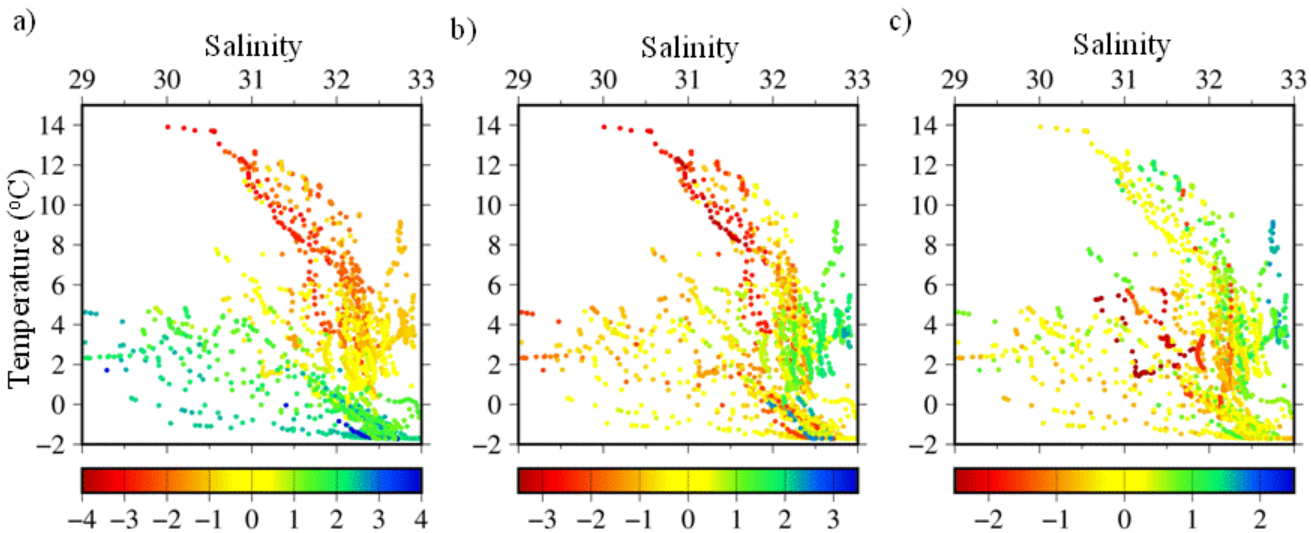

Fig. 2. (Sasaki et al.)

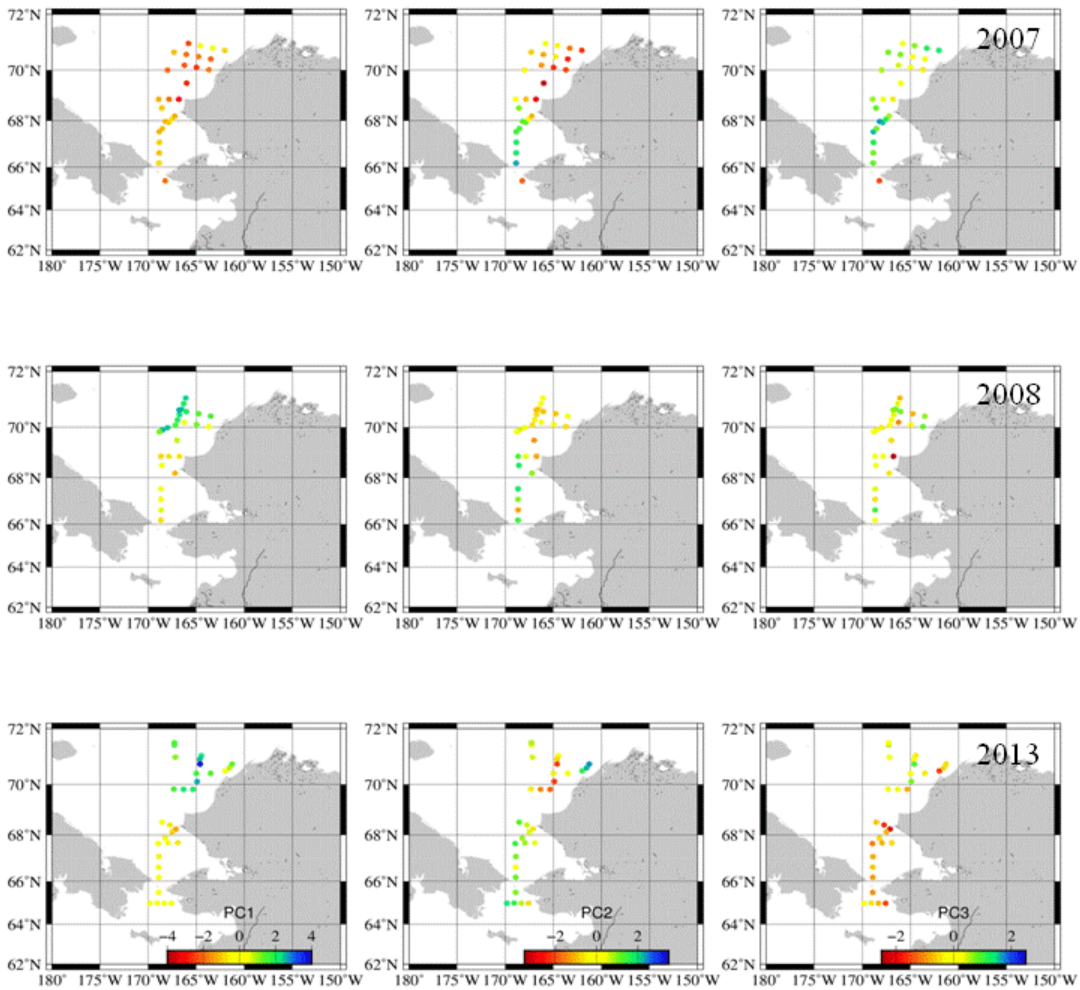

Fig. 3. (Sasaki et al.)

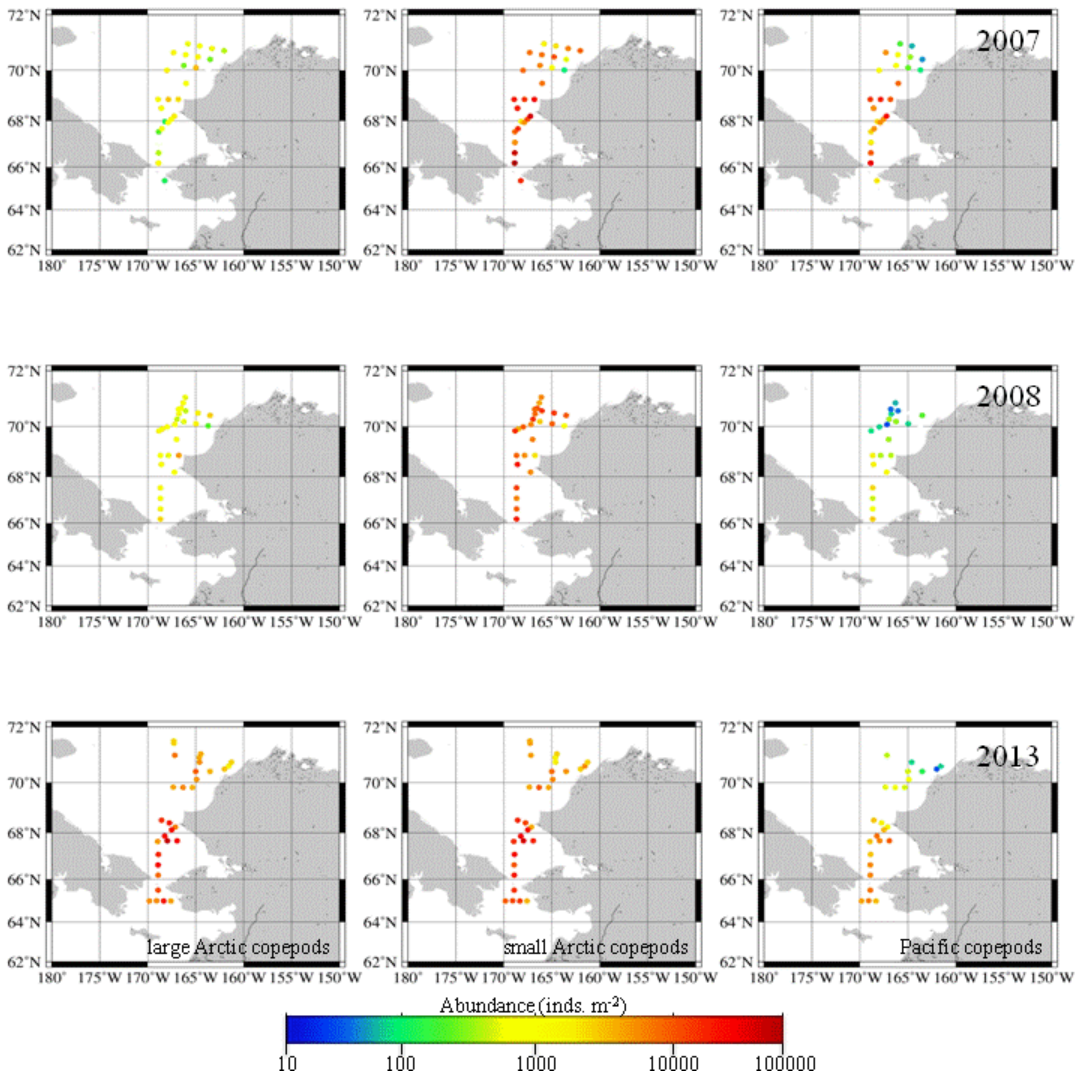

Fig. 4. (Sasaki et al.)

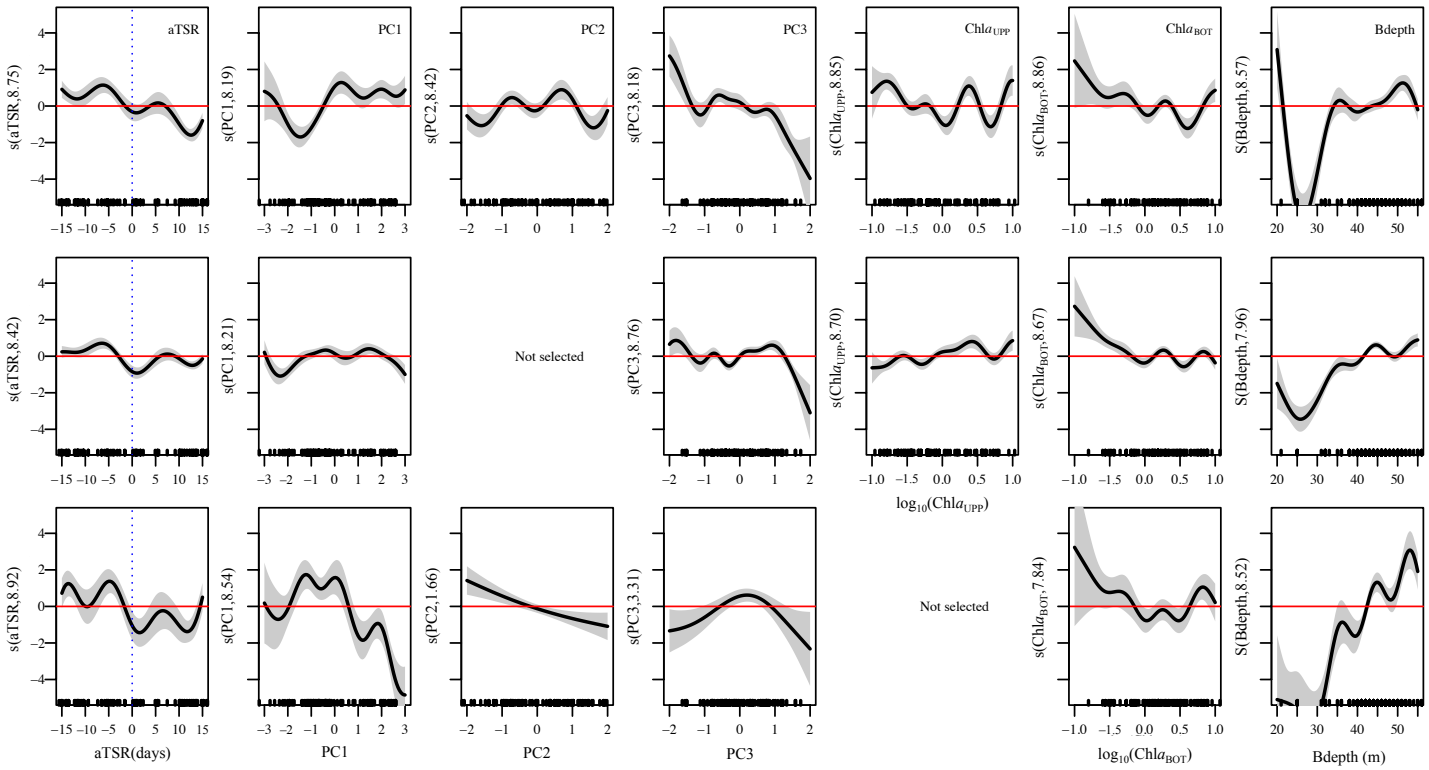

Fig. 5. (Sasaki et. al.)

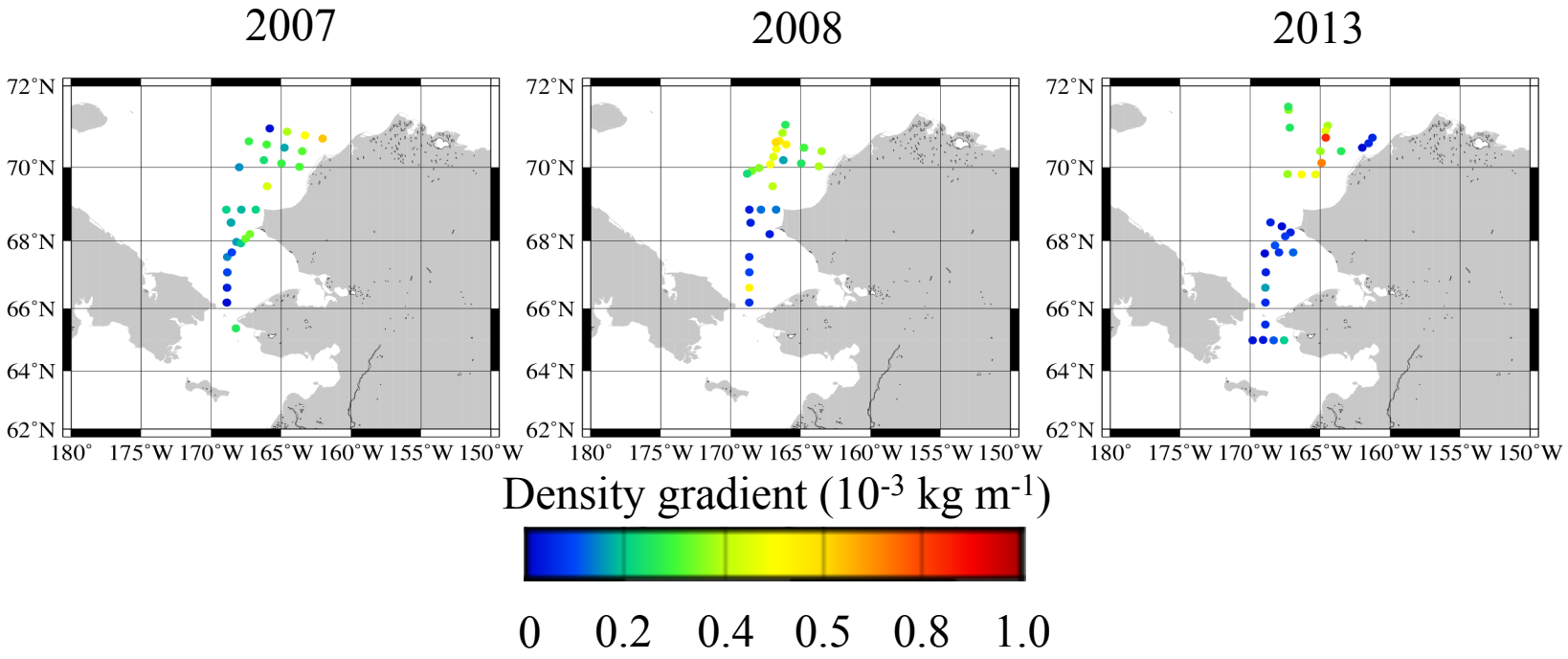
2007
2008
2013
72°N
70°N
68°N
66°N
64°N
62°N
180° 175°W 170°W 165°W 160°W 155°W 150°W
Density gradient (10-3 kg m-1)
0 0.2 0.4 0.5 0.8 1.0

Figure A1.

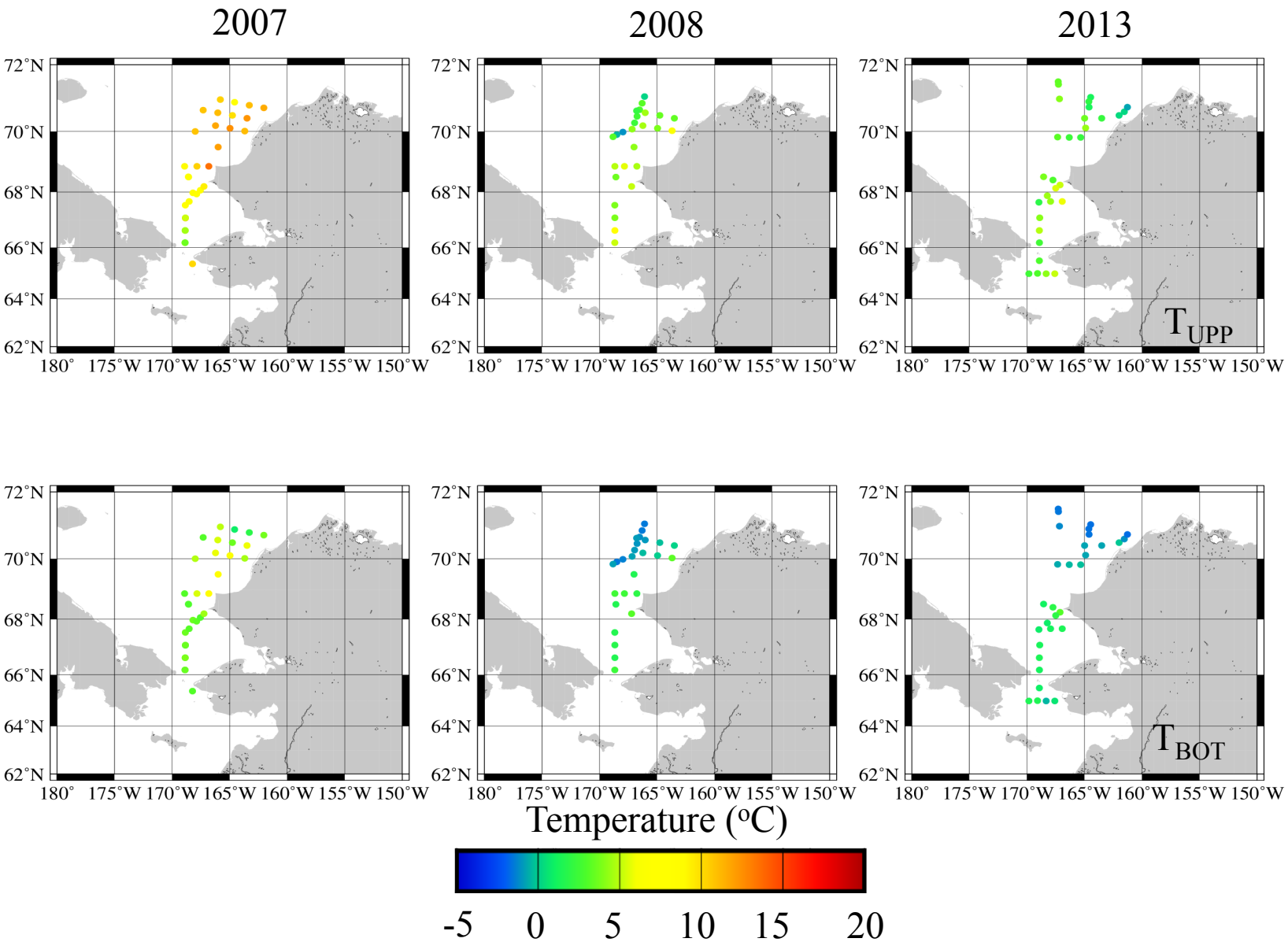
2007
2008
2013
72°N
70°N
68°N
66°N
64°N
62°N
180° 175°W 170°W 165°W 160°W 155°W 150°W
T_{UPP}
T_{BOT}
Temperature (°C)
-5 0 5 10 15 20

Figure A2.

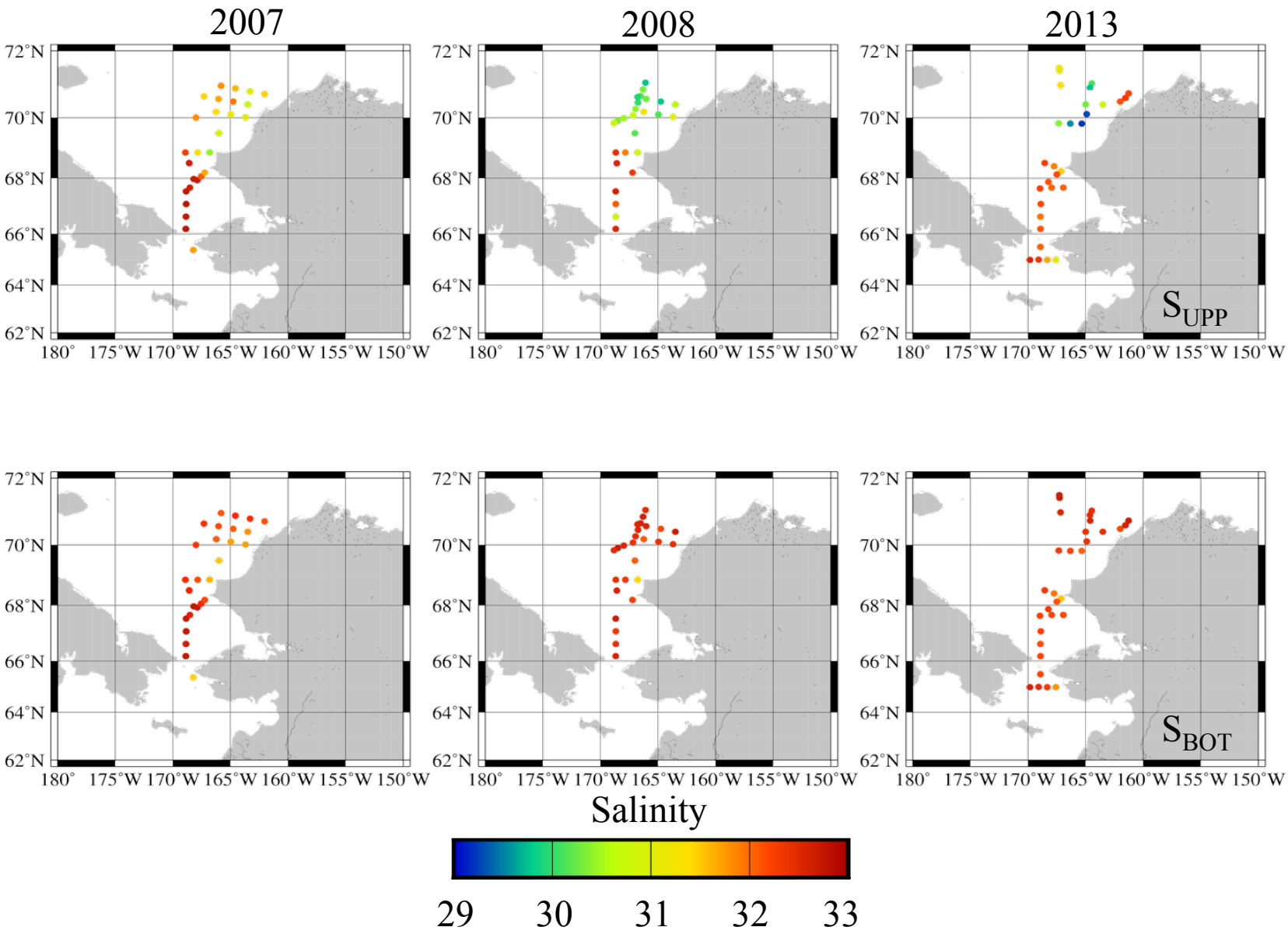
2007
2008
2013
72°N
70°N
68°N
66°N
64°N
62°N
180° 175°W 170°W 165°W 160°W 155°W 150°W
S_{UPP}
S_{BOT}
Salinity
29
30
31
32
33

Figure A3.

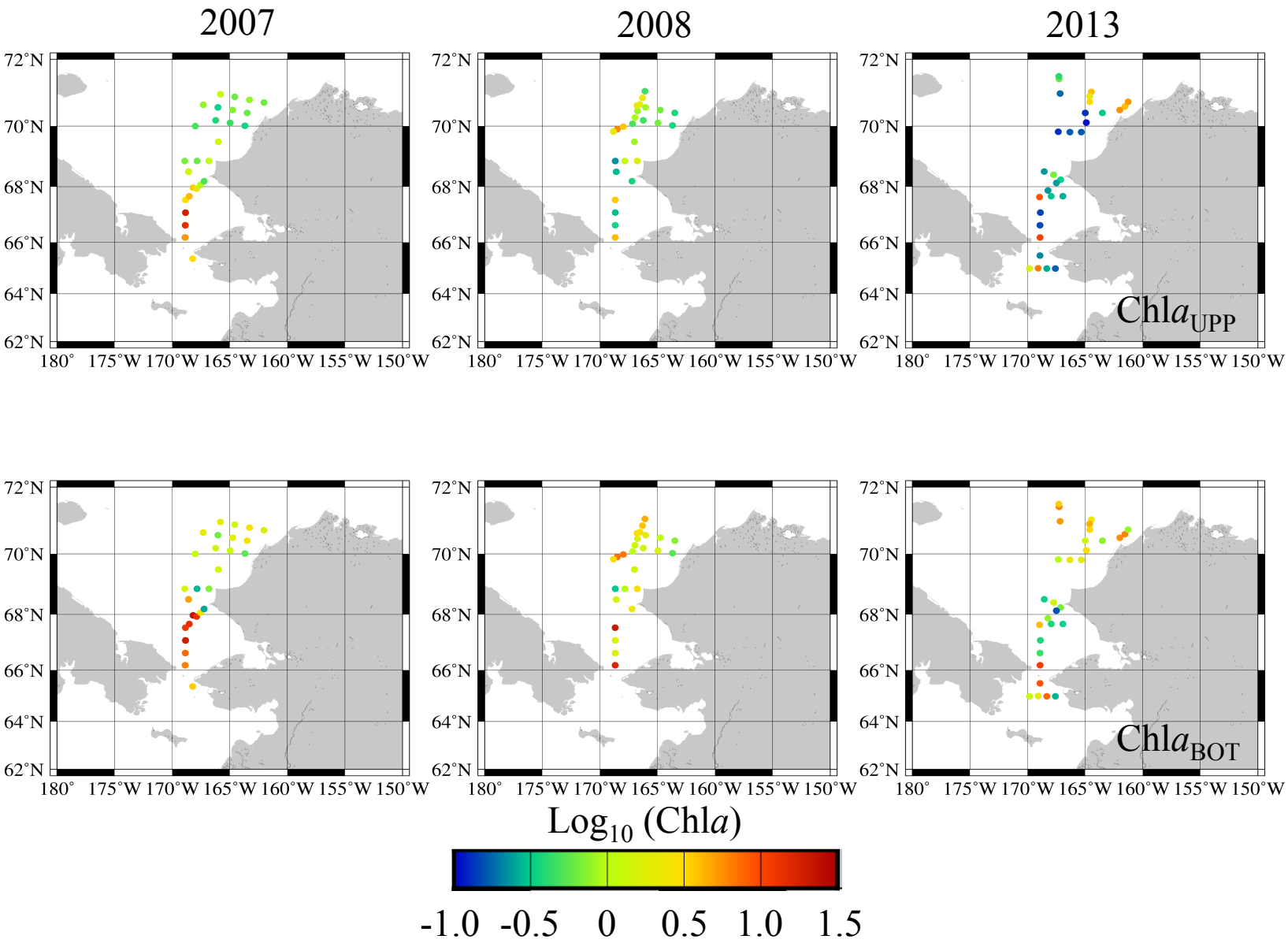
2007
2008
2013
72°N
70°N
68°N
66°N
64°N
62°N
180° 175°W 170°W 165°W 160°W 155°W 150°W
Chla$_{UPP}$
Chla$_{BOT}$
Log$_{10}$ (Chl*a*)
-1.0 -0.5 0 0.5 1.0 1.5

Figure A4.

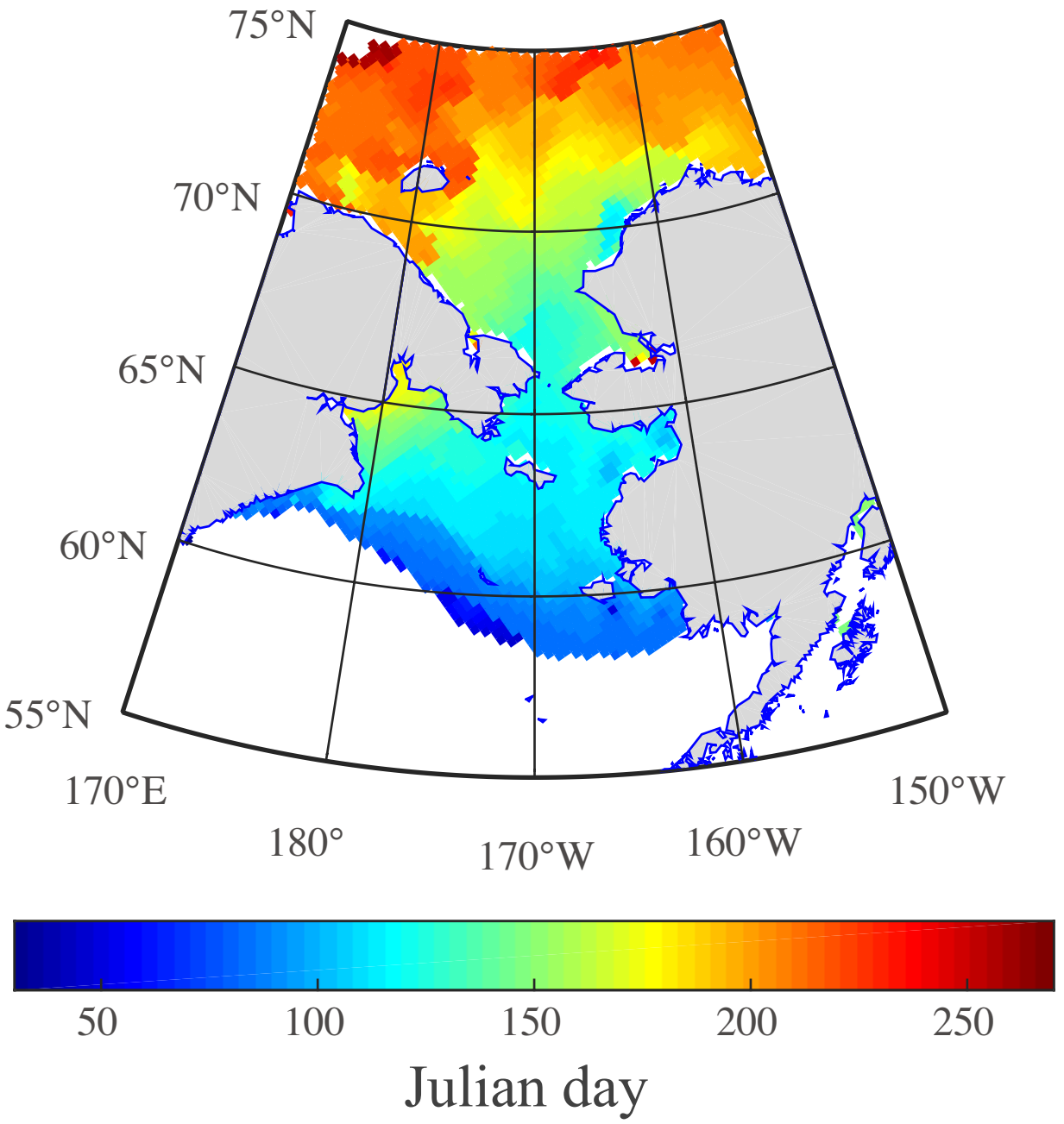
75°N
70°N
65°N
60°N
55°N
170°E
180°
170°W
160°W
150°W
50
100
150
200
250
Julian day

Figure B1

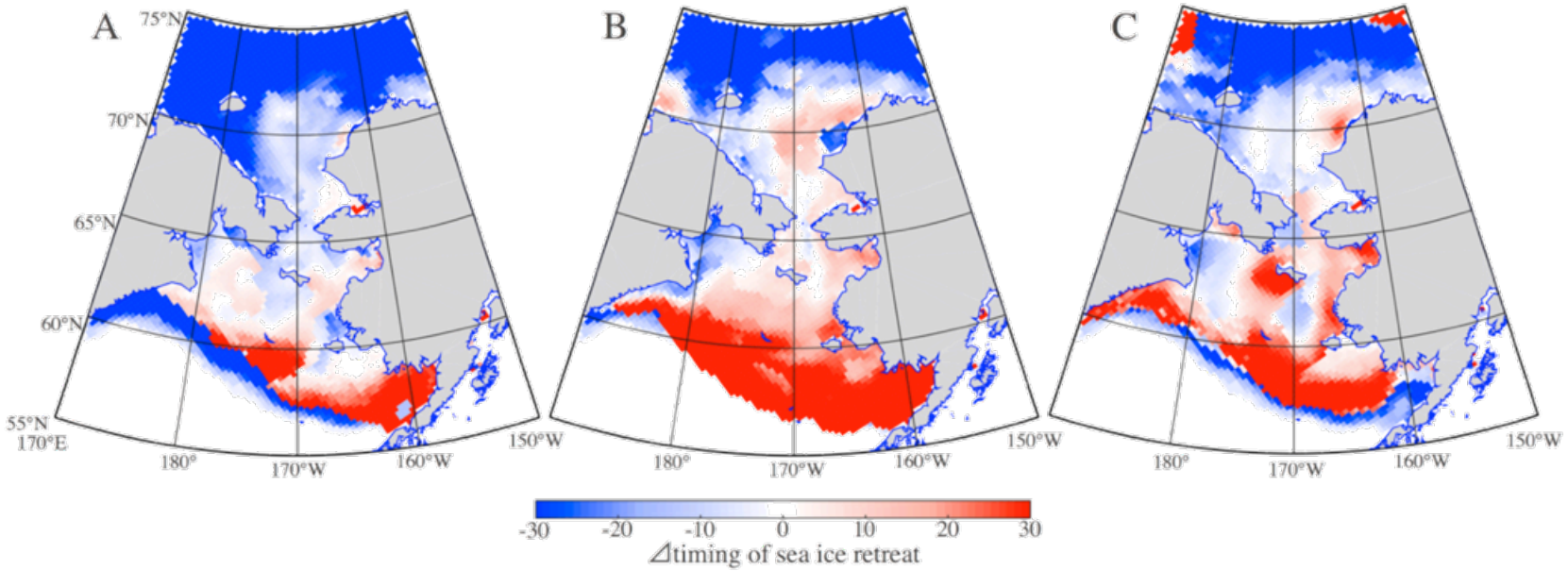
A
B
C
75°N
70°N
65°N
60°N
55°N
170°E
180°
170°W
160°W
150°W
-30
-20
-10
0
10
20
30
⊿timing of sea ice retreat

Figure B2

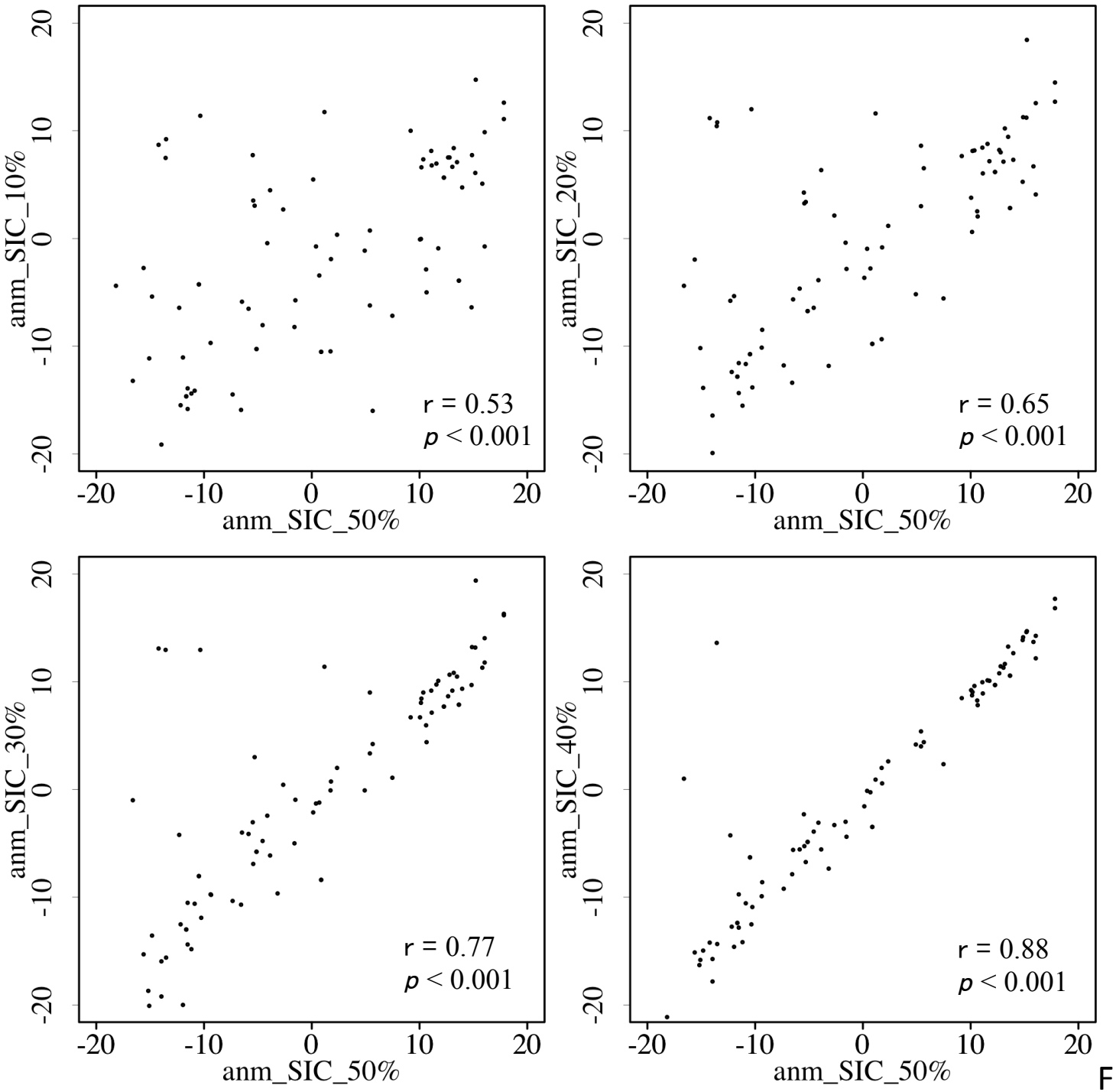
anm_SIC_10%
anm_SIC_50%
r = 0.53
p < 0.001
anm_SIC_20%
anm_SIC_50%
r = 0.65
p < 0.001
anm_SIC_30%
anm_SIC_50%
r = 0.77
p < 0.001
anm_SIC_40%
anm_SIC_50%
r = 0.88
p < 0.001

Figure B3